농학석사학위논문

시아노박테리아 아나베나 유래 두 가지 기능 보유 효소 AgrE의 구조와 기능에 대한 연구

Structural and Functional Analyses of the Bifunctional Enzyme AgrE from the Cyanobacterium *Anabaena*

2020년 8월

서울대학교 대학원

농생명공학부 응용생명화학전공

이 해 희

A Dissertation for the Degree of Master of Science

Structural and Functional Analyses of the Bifunctional Enzyme AgrE from the Cyanobacterium *Anabaena*

August 2020

Haehee Lee

Applied Life Chemistry Major

Department of Agricultural Biotechnology

Seoul National University

Abstract

In cyanobacteria, metabolic pathways for the nitrogen-rich arginine play a crucial role in nitrogen mobilization and storage. An arginine dihydrolase, a member of the guanidine-modifying enzyme (GME) family, was recently characterized in the N-terminal domains of two cyanobacterial enzymes: AgrE from *Anabaena* sp. strain PCC 7120 and ArgZ from *Synechocystis* sp. PCC 6803. These two enzymes catalyze the arginine catabolic pathway and produce an ammonia as well as ornithine and CO_2. In *Synechocystis* sp. PCC 6803, the ornithine–ammonia cycle mediated by ArgZ is responsible for nitrogen remobilization and storage. In AgrE, the C-terminal domain contains additional enzyme, an ornithine cyclodeaminase that converts ornithine into proline and ammonia. Therefore, AgrE is a bifunctional enzyme that performs two sequential reactions for arginine catabolism. In this thesis, the crystal structure of AgrE in a tetrameric conformation is presented, along with three different structures of AgrE, each with a different ligand. These structural data identified the binding sites for the substrate L-arginine and, the product L-ornithine in arginine dihydrolase that has similar features on the structure and catalytic mechanism of a known arginine hydrolase in the GME family. The ternary complex of AgrE containing the coenzyme NAD(H) for ornithine cyclodeaminase and ornithine for arginine dihydrolase suggested a possible passage for substrate channeling that connects the active site of the N-terminal domain to that of the C-terminal domain. Unfortunately, I was unable to detect ornithine cyclodeaminase activity in this study by employing AgrE expressed and purified from *E.coli*. The functional analysis indicated that Asn71 in the active site of arginine dihydrolase is essential for enzyme activity. In particular, the steady-state kinetic analysis showed that the mutant N71D has stronger affinity with the substrate L-arginine compared to the wild-type enzyme.

Key words: *Anabaena* sp. strain PCC 7120, ammonia production, arginine catabolism, bifunctional enzyme, guanidine removing enzyme, nitrogen remobilization, substrate channeling, X-ray crystallography

***Student Number*: 2018-21199**

Table of Contents

List of Tables

List of Figures

List of Abbreviations

DTT	dithiothreitol
NAD(H)	nicotinamide adenine dinucleotide (reduced form)
NADPH	reduced nicotinamide adenine dinucleotide phosphate
PCR	polymerase chain reaction
PDB	protein data bank
SDS-PAGE	sodium dodecyl sulfate–polyacrylamide gel electrophoresis
TCEP	tris(2-carboxyethyl)phosphine

Introduction

Nitrogen is the key element which is incorporated into all living organisms with diverse forms including organic compounds such as amino acids and nucleic acids. Cyanobacteria are the prokaryotes that can perform oxygenic photosynthesis, and many cyanobacteria can convert atmospheric nitrogen into biologically accessible ammonium through nitrogen fixation (Zehr, 2011). Ammonium as a nitrogen source is subsequently incorporated into the carbon skeletons through glutamine synthetase (GS)–glutamate synthase (GOGAT) cycle as the major ammonium assimilation pathway in cyanobacteria (Muro-Pastor et al., 2005), and the resulting glutamine acts as a starting material for the synthesis of many metabolites.

In cyanobacteria, cyanophycin is a polymer (multi-L-arginyl-poly-L-aspartic acid) for nitrogen storage and synthesized as a non-ribosomal polypeptide which consists of arginine and aspartate (Simon, 1973; Simon and Weathers, 1976). Cyanophycin is accumulated under certain conditions including loss of light, CO_2, and starvation of sulfur and phosphorus (Allen et al., 1980). In heterocyst-forming cyanobacteria, vegetative cells under combined nitrogen deprivation differentiate into heterocysts for nitrogen fixation by nitrogenase (Flores and Herrero, 2010). Once the growth condition is recovered, the accumulated cyanophycin in heterocysts is degraded by cyanophycinase (Richter et al., 1999). The resulting dipeptide, β-aspartyl-arginine, is a nitrogen vehicle from cyanophycin, and subsequently transferred into adjacent vegetative cells (Burnat et al., 2014). The dipeptide is further hydrolyzed by isoaspartyl dipeptidase, producing arginine and aspartate (Hejazi et al., 2002).

Arginine as a nitrogen-rich amino acid is mainly responsible for nitrogen redistribution in cyanobacteria (Zhang and Yang, 2019). In *Anabaena* sp. strain PCC 7120, AgrE, an enzyme responsible for arginine catabolism, was recently discovered (Burnat et al., 2019). With proline oxidase PutA in the AgrE-PutA pathway, AgrE is

expressed at a higher level in heterocysts rather than vegetative cells. AgrE catalyzes degradation of arginine to produce ammonia and proline which is converted sequentially by PutA into glutamate (Liu et al., 2017). In AgrE from *Anabaena* sp. strain PCC 7120, its N-terminal region contains arginine dihydrolase that degrades arginine and produces ornithine, CO_2, and two ammonia molecules (Fig. 1A). ArgZ from non-diazotrophic cyanobacteria *Synechocystis* sp. PCC 6803, a possible ortholog of AgrE, was identified as an arginine dihydrolase in an ornithine-ammonia cycle (OAC) that was newly discovered in cyanobacteria (Fig. 1B; Zhang et al., 2018). In the OAC and the GS-GOGAT cycle, the ArgZ-dependent reaction utilizes arginine, resulting in the production of ornithine for nitrogen mobilization and storage in cyanophycin through arginine synthesis. Thus, the arginine catabolism by ArgZ is connected with arginine biosynthetic pathway for its recycling. The C-terminal region of AgrE contains ornithine cyclodeaminase (Fig. 1A; Burnat et al., 2019). In the ornithine cyclodeaminase reaction, ornithine released from N-terminal region is converted into proline with production of one ammonia (Goodman et al., 2004), indicating that AgrE is a bifunctional enzyme responsible for two consecutive reactions in arginine catabolism. The C-terminal region of AgrE was known as a new type of ornithine cyclodeaminase that is homologous to an archaeal protein (Burnat et al., 2019).

In this thesis, I determined the crystal structure of AgrE in different ligation states: an unliganded structure; a ternary compolex with the product of arginine dihydrolase, L-ornithine, and the coenzyme of ornithine cyclodeaminase, NAD(H); and a binary complex with the substrate of arginine dihydrolase, L-arginine. The structural information provides ligand binding sites for arginine dihydrolase and ornithine cyclodeaminase, and the functional study with various mutant enzymes including kinetic analysis provides catalytic insights into arginine dihydrolase. These structural and functional analyses support the proposal that the lateral Asn71 plays a key role for arginine dihydrolase activity. Furthermore, the structural observations also show

a putative tunnel for substrate channeling in AgrE as the bifunctional enzyme. Many contents of this dissertation are recently published in the Journal of Biological Chemistry as myself in the first author (Lee and Rhee, 2020).

Figure 1. Overall reaction scheme and secondary structure of the bifunctional enzyme AgrE

(A) In AgrE, the N-terminal domain shows arginine dihydrolase activity which converts arginine into ornithine, CO_2, two ammonia molecules. Sequentially, the ornithine cyclodeaminase for the C-terminal domain using the released ornithine with coenzyme NAD(H) produces proline and one ammonia molecule. A middle domain between the N- and C-terminal domains is shown in *gray*. The residues for domains were determined according to the structural analysis in this study. (B) The secondary structure of AgrE (WP_010999121) defined in the unliganded form and the amino acid sequence alignment with its homolog ArgZ (WP_010874123) are shown with their high sequence identity. Highly conserved residues are represented in *red* with *blue boxes*, and strictly conserved residues are represented in a *red background*. The figure for the sequence alignment was performed using ESPript (Robert and Gouet, 2014).

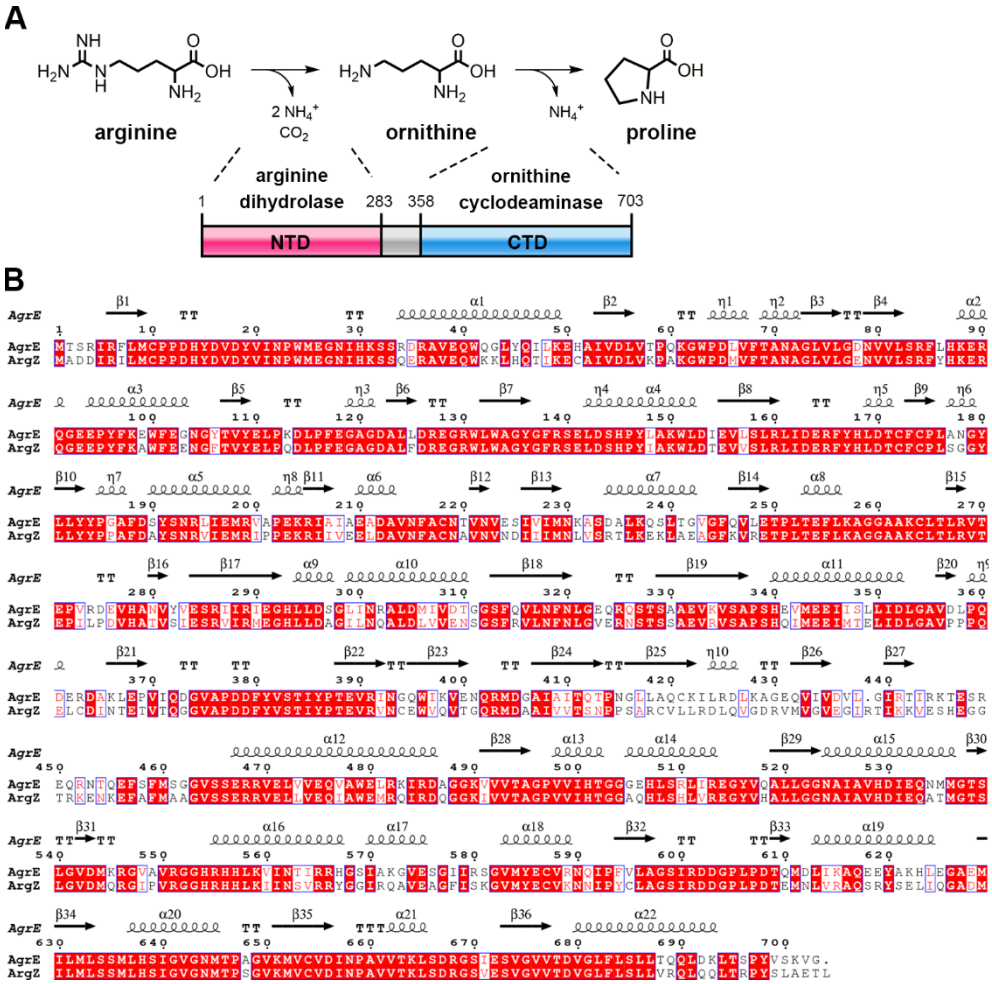
A
arginine
2 NH4+
CO2
ornithine
NH4+
proline
arginine dihydrolase
ornithine cyclodeaminase
1
283
358
703
NTD
CTD
B
AgrE
ArgZ

Materials and Methods

Cloning and purification of AgrE

The full-length AgrE gene for protein crystal was amplified by PCR using the synthetic gene for AgrE (Bioneer, Korea) as a template. The PCR product was cloned into a modified pET-28b vector (Merck, Germany) using two restriction sites, NdeI and XhoI, with a tobacco etch virus protease cleavage site between the His_5 tag and the multiple cloning site. The resulting AgrE plasmid with N-terminal His_5 tag was transformed into *Escherichia coli* BL21 (DE3) cells (Novagen). The AgrE (C264A) mutant for crystallization and the AgrE-NTD (Met1 to Val283) for functional assay were cloned and amplified by PCR using the full-length AgrE gene as a template. Also, DNAs for various AgrE-NTD mutants were amplified by site-directed mutagenesis using the AgrE-NTD as a template with specific mutagenic primers (Table 1).

For crystallization, *E.coli* cells were cultured at 37℃ in LB medium containing 50 μg/ml kanamycin until the optical density at 600 nm reached 0.4–0.6. Then overexpression of AgrE was induced by 0.5 mM IPTG, and the *E.coli* cells were further incubated at 20℃ overnight. The collected cells were sonicated and centrifuged in buffer A (50 mM Tris, pH 8.0, 100 mM NaCl, 2 mM $MgCl_2$, and 2 mM DTT). Next, the AgrE protein was purified by a HisTrap HP column (GE Healthcare) for affinity chromatography with buffer A and buffer B (buffer A plus 500 mM imidazole) for elution (Fig. 2A). The N-terminal His_5 tag of AgrE was subsequently removed during dialysis with buffer A overnight at 4℃ using tobacco etch virus protease. The His tag-free AgrE protein was purified by additional affinity chromatography using buffer A, followed by size-exclusion chromatography using a Superdex-200 column (GE Healthcare) with a buffer (0.1 M imidazole, pH 8.0) (Fig. 2, B and C). The AgrE protein in each purification step was confirmed by SDS-PAGE

(Fig. 2D). For structural analysis, a seleno-L-methionine (SeMet)–substituted AgrE with N-terminal His_5 tag expressed in *E.coli* BL21 (DE3) cells was cultured in M9 minimal medium supplemented with SeMet as previously described (Van Duyne et al., 1993). Furthermore, for the enzyme assay, full-length AgrE, AgrE-NTD, and its various mutants with N-terminal His_5 tag were purified by HisTrap HP column, followed by HiPrep 26/10 column (GE Healthcare) for desalting procedure with a buffer containing 50 mM Tris, pH 8.0, and 300 mM NaCl. I confirmed that the features of these mutants during purification procedures were the same as those of AgrE-NTD via size-exclusion chromatography and SDS-PAGE (Fig. 3).

Table 1. Primers for AgrE and arginine deiminase.

Primers for the full-length of AgrE	
Forward	TTTCAGGGCCATATGACCTCCCGTATCCGTTTCC
Reverse	GTGGTGGTGCTCGAGTTAACCCACCTTAGAAACG
Primers for AgrE-NTD	
Forward	TTTCAGGGCCATATGACCTCCCGTATCCGTTTCC
Reverse	GTGGTGGTGCTCGAGTTACACGTAGACGTTCGCG
Primers for various mutants of AgrE	
N22A_F	CGTGATT**GCG**CCATGGATGGAAGGCAACATC
D65A_F	GTGGCCG**GCG**CTCGTCTTTACCGCTAACGCG
N71A_F	TACCGCT**GCG**GCGGGTCTGGTTCTCGGCGAT
N71D_F	TACCGCT**GAT**GCGGGTCTGGTTCTCGGCGAT
R90A_F	CAAAGAG**GCG**CAGGGTGAAGAACCGTATTTT
E118A_F	GCCGTTC**GCG**GGCGCCGGTGATGCGCTGCTG
D122A_F	CGCCGGT**GCG**GCGCTGCTGGATCGCGAGGGC
D122N_F	CGCCGGT**AAC**GCGCTGCTGGATCGCGAGGGC
R139A_F	CGGCTTC**GCG**TCCGAACTGGATTCTCATCCG
Y167F_F	ACGTTTT**TTT**CACCTGGATACTTGTTTTTGT
H168A_F	TTTTTAC**GCG**CTGGATACTTGTTTTTGTCCG
D170A_F	CCACCTG**GCG**ACTTGTTTTTGTCCGCTGGCA
D170N_F	CCACCTG**AAC**ACTTGTTTTTGTCCGCTGGCA
N219A_F	CGCCTGT**GCG**ACCGTTAATGTCGAGTCTATC
C264A_F	GGCAAAA**GCG**CTGACCCTGCGCGTGACTGAA
Primers for arginine deiminase from genomic DNA of *Pseudomonas aeruginosa*	
Forward	TTTCAGGGCCATATGAGCACGGAAAAAACCAAAC
Reverse	GTGGTGGTGCTCGAGTCAGTAGTCGATCGGGTCG

The direction of sequences is described from 5' to 3'. For various mutants of AgrE, only forward primers are listed. Bold-underlined sequences represent codon substitution for mutation.

Figure 2. Elution profiles and the SDS-PAGE gel of full-length AgrE during its purification for crystallization

(A–C) On elution profiles, *blue line* shows the protein absorbance at 280 nm, and *green line* shows the imidazole concentration (%) in buffer for elution. (A) After cell lysis, the His_5-tagged AgrE was purified by immobilized metal affinity chromatography (IMAC). (B) Purification for His tag-free AgrE was performed in the second IMAC following elimination of N-terminal His_5 tag. (C) Size-exclusion chromatography was carried out for higher purity of the His tag-free AgrE enzyme. (D) Protein samples for each purification procedures were used in SDS-PAGE with a 14% separating gel. Each number is consistent with that of the elution peak. M, protein marker; T, total protein following cell lysis; S, soluble protein corresponding to supernatant after centrifugation; C, the concentrated AgrE purified by size-exclusion chromatography. (AgrE : 78 kDa)

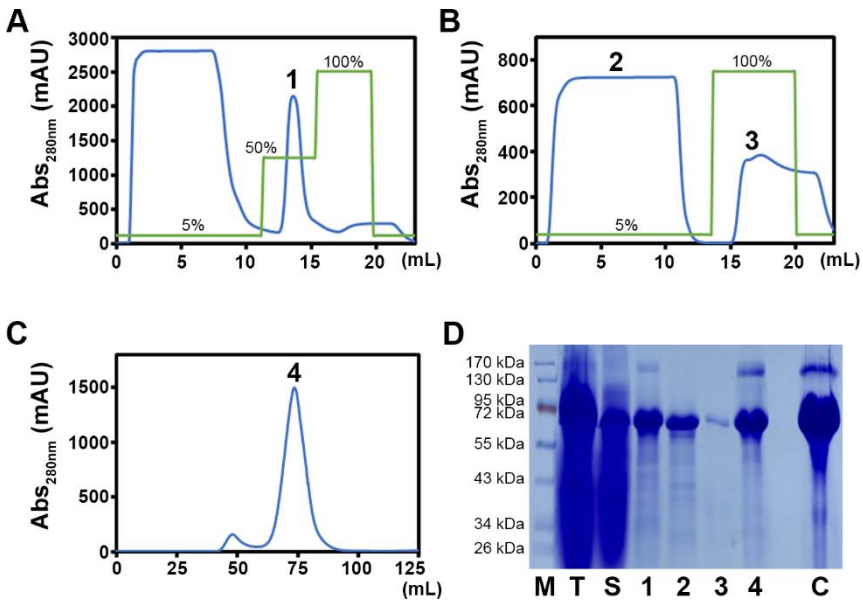
A
B
C
D
Abs280nm (mAU)
(mL)
100%
50%
5%
1
2
3
4
170 kDa
130 kDa
95 kDa
72 kDa
55 kDa
43 kDa
34 kDa
26 kDa
M T S 1 2 3 4 C

Figure 3. Elution profiles and the SDS-PAGE gel of AgrE-NTD with its mutants for functional analysis

(A) After cell lysis, the His_5-tagged AgrE-NTD was purified by IMAC. *Blue line* shows the protein absorbance at 280 nm, and *green line* shows the imidazole concentration (%) in buffer for elution. (B) The AgrE-NTD and its several mutants used for the kinetic analysis were purified by size-exclusion chromatography for the verification of their stable protein folding in solution. (C) For functional analysis, the AgrE-NTD and its mutants for 12 residues were analyzed by SDS-PAGE with a 14% separating gel following the desalting procedure. (AgrE-NTD : 32 kDa)

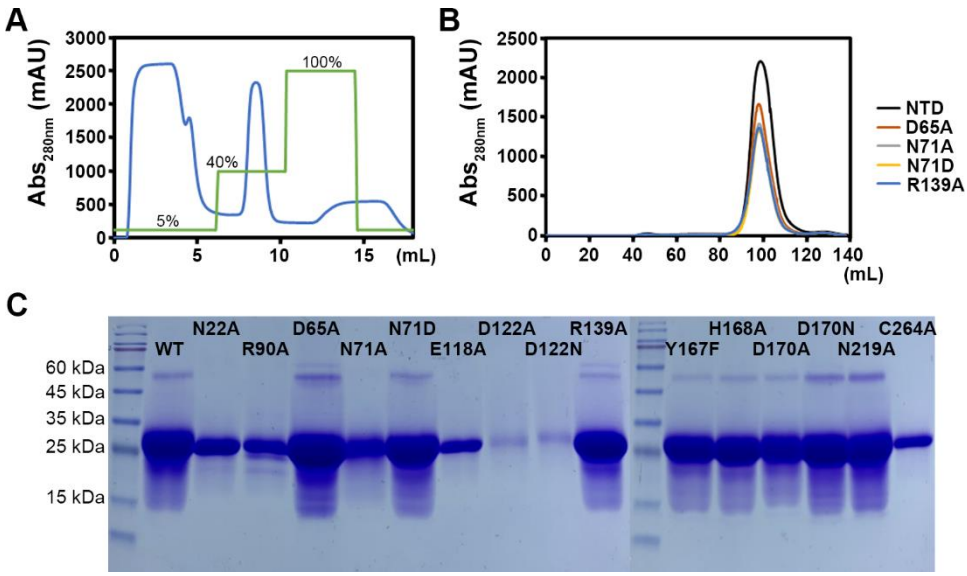
A
Abs280nm (mAU)
3000
2500
2000
1500
1000
500
0
100%
40%
5%
0
5
10
15
(mL)
B
Abs280nm (mAU)
2500
2000
1500
1000
500
0
0
20
40
60
80
100
120
140
(mL)
NTD
D65A
N71A
N71D
R139A
C
WT
N22A
R90A
D65A
N71A
N71D
E118A
D122A
D122N
R139A
H168A
Y167F
D170A
D170N
N219A
C264A
60 kDa
45 kDa
35 kDa
25 kDa
15 kDa

Crystallization and structure determination

For crystallization of three AgrE structures, each purified protein was concentrated in a buffer containing 100 mM imidazole, pH 8.0. Then the protein crystallization was carried out using a crystallization solution containing 0.2 M sodium acetate, 0.1 M sodium citrate, pH 5.5, 10% (w/v) PEG 4000, and 5% (v/v) glycerol at 22℃ by the sitting-drop vapor diffusion method (Fig. 4A). Purified SeMet–substituted AgrE for unliganded structure was concentrated to 10.7 mg/ml, and the crystal was achieved using the crystallization solution in addition to 10 mM TCEP. The binary complex with arginine was produced by co-crystallizing 5 mM arginine with purified AgrE (C264A) mutant concentrated to 5.9 mg/ml. The ternary complex with ornithine and NAD^+ was generated by soaking the native AgrE crystal at a concentration of 10.8 mg/ml in the crystallization solution with 5 mM ornithine and 5 mM NAD^+ for 20 min.

On Beamline 7A and 11C at the Pohang Accelerator Laboratory (Korea), x-ray diffraction data were collected with an oscillation angle of 0.5˚ (Fig. 4B). For the data collection achieved at 100K, the crystals were soaked in the crystallization solution with additional 20% (v/v) ethylene glycol as a cryoprotectant. The collected data were processed by HKL2000 (Otwinowski and Minor, 1997), with the high-resolution cutoff based on a $CC^1/_2$ statistical value of approximately 0.5 (Winn et al., 2011; Karplus and Diederichs, 2012; Diederichs and Karplus, 2013). The space group of all crystals was $C222_1$, with two monomers in the asymmetric unit (Table 2).

The structure of unliganded SeMet–substituted AgrE was solved by the PHENIX program (Zwart et al., 2005; Adams et al., 2010) using single-wavelength anomalous dispersion data for phase calculation. Rounds of manual model fitting were conducted using the COOT program (Emsley et al., 2010), and subsequent refinement was performed by PHENIX. The ternary structure and the binary structure were determined using the structure of unliganded SeMet–substituted AgrE

as a starting model. During refinement, the electron density corresponding to ornithine and NAD^+ in ternary complex and arginine in the active site of the binary complex was clearly observed on the F_o–F_c map. More details of the data collection and refinement statistics are listed in Table 2.

Figure 4. Crystals and diffraction image of AgrE

(A) Crystals of AgrE were grown under 0.2 M sodium acetate, 0.1 M sodium citrate, pH 5.5, 10% (w/v) PEG 4000, 5% (v/v) glycerol, and 10 mM TCEP. (B) Diffraction image of AgrE.

A

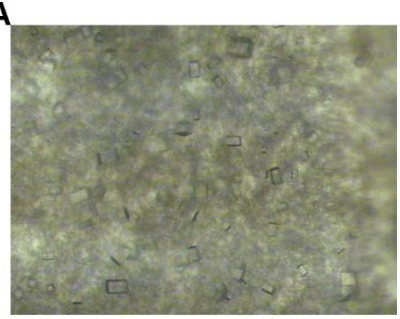

B

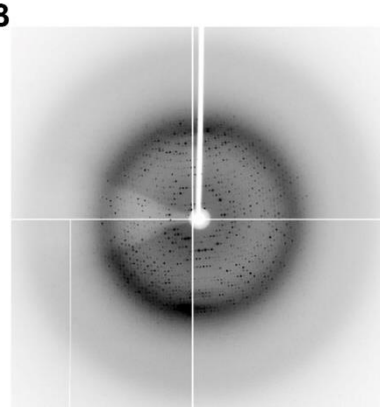

Table 2. Data collection and refinement statistics.

Data set	Unliganded AgrE	AgrE in complex with L-ornithine and NAD(H)	AgrE in complex with L-arginine
PDB ID	6LRF	6LRG	6LRH
Data collection			
Wavelength (Å)	0.9792	0.9795	0.9795
Resolution (Å)	50.0-2.05(2.12-2.05)[a]	50.0-2.40 (2.49-2.40)	50.0-2.70(2.80-2.70)
Unique reflections	114,936 (10,839)	71,345 (7,051)	50,860 (5,040)
Multiplicity	6.6 (5.8)	5.8 (5.7)	6.6 (5.8)
Completeness (%)	98.2 (93.4)	99.0 (99.2)	99.8 (99.5)
Mean I/sigma(I)	12.2 (1.9)	9.8 (3.0)	7.5 (1.8)
Wilson *B*-factors (Å^2)	25.9	28.7	33.7
R-merge	0.182 (1.09)	0.261 (1.45)	0.247 (0.985)
$CC_{1/2}$[b]	0.989 (0.437)	0.991 (0.835)	0.985 (0.832)
Space group	*C222$_1$*	*C222$_1$*	*C222$_1$*
Unit cell			
a, b, c (Å)	187.6, 201.7, 99.6	186.9, 201.1, 99.4	186.2, 201.5, 99.0
α , β , γ (º)	90, 90, 90	90, 90, 90	90, 90, 90
Refinement			
R-work[c]	0.209	0.192	0.193
R-free[d]	0.247	0.251	0.245
No. of atoms			
Macromolecules	10552	10605	10451
Ligands	0	62	24
Water	441	132	44
RMS(bonds) (Å)	0.009	0.009	0.011
RMS(angles) (º)	1.12	1.18	1.16
Ramachandran			
favored (%)	96.6	95.6	94.8
outliers (%)	0.2	0.4	0.2
Average *B*-factors (Å^2)	31.6	33.2	23.0
Macromolecules	31.5	33.2	23.0
Ligands		41.7	12.7
Water	33.3	31.0	18.7

[a]Numbers in parentheses refer to data in the highest resolution shell.
[b]The CC1/2 is the Pearson correlation coefficient (CC) calculated from each subset containing a random half of the measurements of unique reflection
[c]$R_{work} = \Sigma \, ||F_{obs}|-|F_{cal}|| / \Sigma |F_{obs}|$
[d]R_{free} is the same as R_{obs} for a selected subset (5%) of the reflections that was not included in prior refinement calculations.

Enzyme activity assays of AgrE and mutants

I carried out activity assay of AgrE using an ammonia assay kit including glutamate dehydrogenase (AA0100, Sigma, USA). In brief, the product ammonia liberated from the AgrE-dependent reaction is involved in the NADPH-dependent glutamate dehydrogenase reaction that converts α-ketoglutarate into glutamate, thereby decreasing the absorbance at 340 nm (Tocilj et al., 2005). The molar extinction coefficient of NADPH is 6,220 $M^{-1} \cdot cm^{-1}$ at 340 nm, and the AgrE activity was identified by measuring changes of absorbance at 340 nm.

The reaction was conducted at 25℃ using a UV-visible spectrophotometer (Jasco, Japan). The pre-reaction mixture included 3 mM α-ketoglutarate, 0.2 mM NADPH, 13 units/mL of glutamate dehydrogenase, and a given concentration of AgrE enzyme. After incubation of the pre-mixture for 150 sec, the reaction was initiated by adding arginine as a substrate of AgrE-NTD. The initial velocity was measured by converting the absorbance changes for 30 sec in the reaction into the amount of corresponding ammonia by using a standard curve (Fig. 5). I confirmed that concentrations of all components including the coupling enzyme (*i.e.* glutamate dehydrogenase) except AgrE enzyme in this assay was present in a saturating condition. Therefore, the initial velocity measured in this assay was determined only by the concentration of AgrE. The kinetic values, K_m and k_{cat}, were calculated using SigmaPlot software (Systat software, USA).

Figure 5. Standard curve for ammonia in NADPH-dependent reaction

(A) The decreasing absorbance at 340 nm was monitored according to given concentrations of ammonia with 0, 6.25, 12.5, 25, 50, 100, or 190 μM in the NADPH-dependent reaction using 13 units/mL of glutamate dehydrogenase. (B) The standard curve for ammonia was calculated by differences of absorbance at 340 nm corresponding to ammonia concentrations. I confirmed a linearity of the standard curve in the reaction condition over a range of 0–190 μM ammonia.

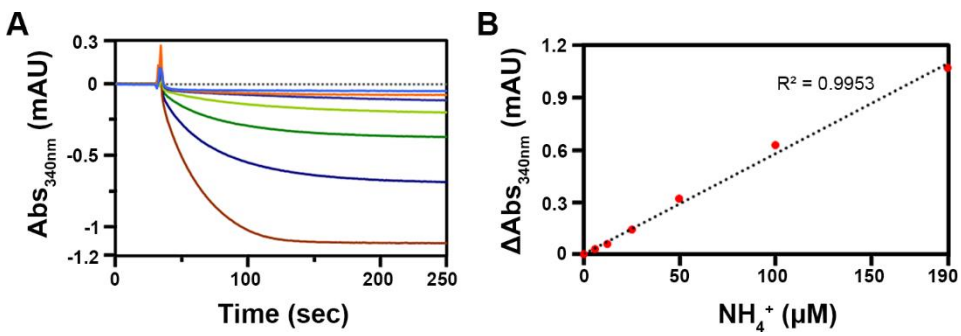
A
0.3
0
-0.5
-1
-1.2
Abs340nm (mAU)
0
100
200
250
Time (sec)
B
1.2
0.9
0.6
0.3
0
ΔAbs340nm (mAU)
R² = 0.9953
0
50
100
150
190
NH4+ (μM)

Result

Overall structure of unliganded AgrE

The structure of AgrE in apo form was determined at 2.05 Å resolution. The two monomers of AgrE were arranged with a non-crystallographic 2-fold symmetry in the asymmetric unit (Fig. 6A). According to an root mean square deviation (RMSD) of 0.91 Å for 665 C_α atoms, the structures of the two monomers are identical. In the crystal, however, the two dimers formed a tetrameric conformation by crystallographic symmetry (Fig. 6B). In addition to size-exclusion chromatography (Fig. 7), PISA assembly analysis (Krissinel and Henrick, 2007) revealed that AgrE protein is present as a tetramer with 222-fold symmetry in solution.

The monomeric structure of AgrE has three domains based on the structural analysis achieved in this study (Fig. 1 and 8A). The N-terminal domain (AgrE-NTD; Met1 to Val283) is arginine dihydrolase. It exhibits high structural similarity, but low sequence identity with other proteins in guanidine-modifying enzyme (GME) family that has its common features (Linsky and Fast, 2010). The AgrE-NTD shows a five–β/α propeller fold and a central hollow on the propeller axis which is involved in substrate binding (Fig. 8B). The DALI search (Holm and Laakso, 2016) revealed that the structure of AgrE-NTD is highly similar with three enzymes in the GME family including dimethylarginine dimethylaminohydrolase (PDB ID 1H70) (Murray-Rust et al., 2001), succinylarginine dihydrolase (PDB ID 1YNI) (Tocilj et al., 2005), and arginine deiminase (PDB ID 1RXX) (Galkin et al., 2004).

The C-terminal domain (AgrE-CTD; Leu358 to Gly703) is the most related to lysine-oxoglutarate reductase/saccharopine dehydrogenase from *Methanococcus maripaludis* (PDB ID 3C2Q) with the ornithine cyclodeaminase activity equivalent to that of the AgrE-CTD. There are two subdomains in the AgrE-CTD which are connected via a loop. It is a disordered region including Lys445 to Gly463 of one

subunit and Arg454 to Gly463 of the other subunit in the asymmetric unit (Fig. 8C). The smaller subdomain, ranging from Leu358 to Arg445, consists of seven β-stranded folds, and the larger subdomain has a Rossmann fold with a α/β domain which ranges from Val464 to Gly703. In the Rossmann fold, six parallel β-strands form a central β-sheet (32-29-28-34-35-36), surrounded by three α-helices on one side and eight α-helices on the other side facing the AgrE-NTD.

Between the N-terminal and C-terminal domains of AgrE, a middle domain (Glu284 to Asp357) consists of three β-strands and two α-helices. The middle domain protrudes from the two domains, making them close to each other. Also, the middle domain of each subunit form a dimerization region which is composed of six β-strands and four α-helices (Fig. 6A). In a tetramer, two dimerization regions for each dimer are located on opposite sides of the center containing four AgrE-CTDs (Fig. 6B).

Figure 6. Dimeric configuration of AgrE and its tetrameric assembly

(A) Dimeric AgrE in the asymmetric unit of the crystal is shown with 2-fold symmetry. The two monomeric AgrE-NTDs are rotated through ~180˚ with each other. In the zoomed-in view, the dimerization is mediated by the protruding middle domains with six-stranded β-sheet and four α-helices. (B) The tetrameric assembly of AgrE exhibits 222-symmetry along the three perpendicular axes. The orientation is obtained following rotation of Fig. 6A through ~90˚ along the vertical axis, and other two AgrE-CTDs of the second dimer are added between the two AgrE-CTDs of the first dimer for tetramerization. Therefore, in the tetramer, the four AgrE-NTDs are located at each end of the central region which consists of the AgrE-CTDs. Each subunit is represented by different colors.

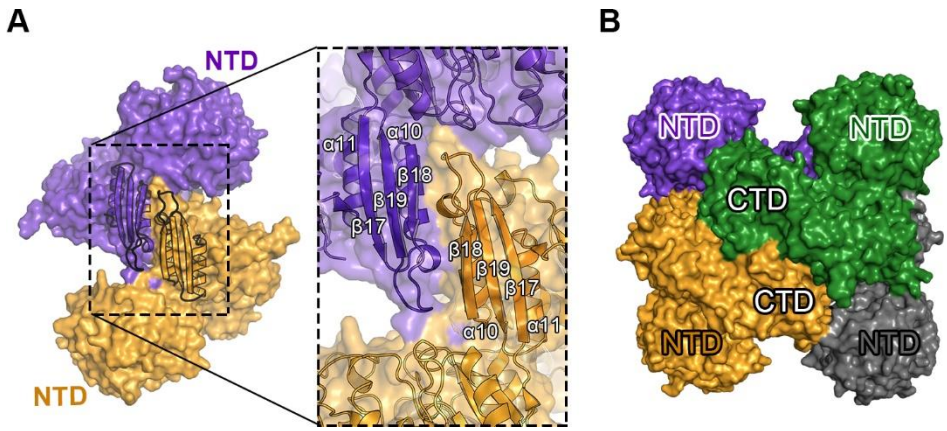
A
NTD
NTD
α11
α10
β18
β19
β17
β18
β19
β17
α10
α11
B
NTD
NTD
CTD
CTD
NTD
NTD

Figure 7. Size-exclusion chromatography analysis of AgrE

The full-length AgrE was purified by analytical size-exclusion chromatography using a Superdex 200 column (GE Healthcare) in a buffer (100 mM imidazole, pH 8.0). The molecular mass of AgrE was calculated by comparing 43–669 kDa molecular mass makers (GE Healthcare). Note that the eluted peak for AgrE at 12.2 mL corresponds to 312 kDa as a tetrameric enzyme. A void volume for the column in this condition was 9.5 mL.

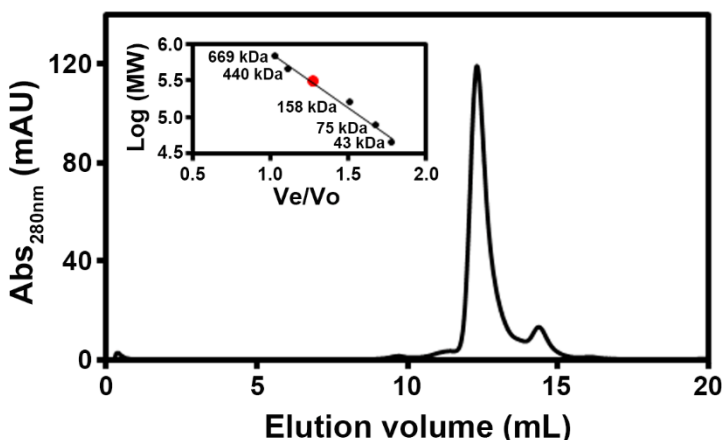
Abs280nm (mAU)
120
80
40
0
0
5
10
15
20
Elution volume (mL)
Log (MW)
6.0
5.5
5.0
4.5
0.5
1.0
1.5
2.0
Ve/Vo
669 kDa
440 kDa
158 kDa
75 kDa
43 kDa

Figure 8. Monomeric structure of the unliganded AgrE

(A) Monomeric AgrE is showed in an L shape. The each domain is represented in different colors. The AgrE-NTD (*red*) is perpendicular to the AgrE-CTD (*blue*), forming an L shape. The middle domain (*purple*) responsible for dimerization protrudes from the NTD and CTD. (B) The AgrE-NTD for arginine dihydrolase includes five β/α-propeller folds in pseudosymmetry. The loop in *blue* connecting α1 and β1 covers the central hollow. (C) The AgrE-CTD for ornithine cyclodeaminase includes two subdomains. The *dashed line* shows a missing loop disordered between the two subdomains.

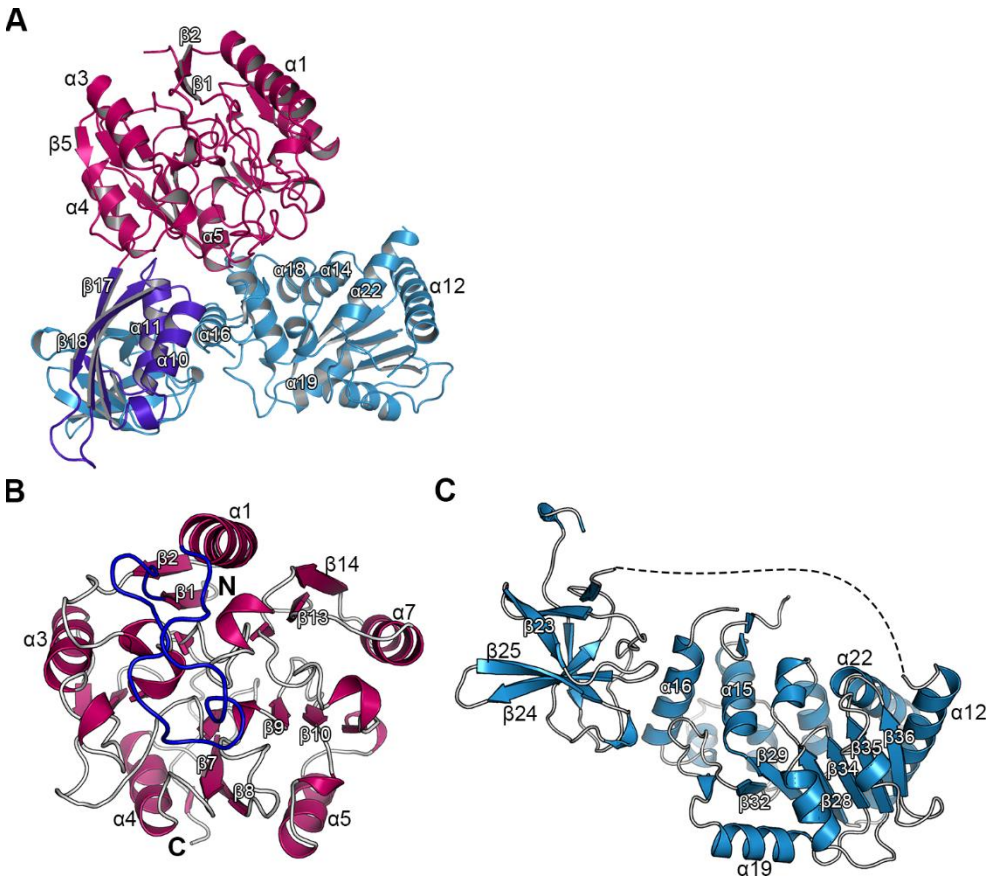
A
β2
α1
α3
β1
β5
α4
α5
α18
α14
α12
β17
α22
α11
α16
β18
α10
α19
B
α1
β2
β14
N
β1
β13
α7
α3
β9
β10
β7
β8
α4
α5
C
C
β23
β25
α22
α16
α15
α12
β24
β29
β36
β35
β34
β32
β28
α19

Active site and catalytic mechanism of AgrE-NTD

The two structures of AgrE complexed with L-ornithine and L-arginine in the NTD were determined at 2.4 Å and 2.7 Å resolution, respectively. The binary complex with L-arginine was observed in the AgrE (C264A) mutant, and the position of other residues in the active site of two structures was identical except for Cys264. The product of the AgrE-NTD, L-ornithine, was in the central hollow of the five-propeller fold (Fig. 9A). The carboxyl- and amino groups of its main chain were present near the entrance close to the AgrE-CTD. The location of L-ornithine and L-arginine was equivalent based on their main chains. Furthermore, the ternary structure with L-ornithine and NAD^+ was almost identical with unliganded AgrE according to 0.36 Å RMSD for 1,351 C_α atoms, indicating that there were no notable conformational changes. Also, in all states, a loop containing Cys10 to Ser33 was observed to cover the entrance of the hollow (Fig. 1B and 8B). In addition to Asn22 on the loop, Asp65, Arg90, and Arg139 stabilized the α-carboxyl group and α-amino group of L-arginine via hydrogen bonds, and the L-arginine was located between Tyr167 and Phe68 within ~4.3 Å. Unlike the ternary complex, Asp170 as an anterior residue mediated the hydrogen-bond interaction with NH1 and NH2 of guanidine group of L-arginine in the binary complex (Fig. 9B).

The GME family has common structural features including a catalytic triad in the active site. For a structural description, I followed the nomenclature of key residues that have been defined for the GME family, and the catalytic mechanism of this enzyme family has been proposed previously (Linsky and Fast, 2010). In the AgrE-NTD, Cys264, His168, and Glu118 act as a catalytic triad. While core Cys264 functions as a nucleophile, core His168 serves as an acid/base catalyst for releasing ammonia and activating water molecule, and Glu118 stabilizes the core histidine via a hydrogen bond. His168 and Glu118 were localized on the other side to Cys264 (Fig. 9B). The catalysis is initiated by a nucleophilic attack of core Cys264 on the CZ atoms in the guanidine group, followed by forming a tetrahedral adduct

covalently bound to the enzyme. Subsequently, the tetrahedral adduct collapses via cleavage of CZ–NH1 bond, and one molecule of ammonia is released from the L-arginine. In case of arginine deiminase (ADI) that has hydrolase activity (Galkin et al., 2004), citrulline is produced through this mechanism with the addition of one water molecule. However, for the reaction of the AgrE-NTD as arginine dihydrolase, there are additional rounds of hydrolysis for breakage of CZ–NH2 bond and NE–CZ bond, resulting in two molecules of ammonia, CO_2, and ornithine. It has been first proposed that a lateral asparagine plays an essential role for dihydrolase activity in the structural study of *N*-succinylarginine dihydrolase (Tocilj et al., 2005). In a hydrolase, a lateral aspartate forms two hydrogen bonds with the NE and NH2 atoms, showing stronger interactions rather than the lateral residue of dihydrolase. The presence of an aspartate at the lateral position would be responsible for the production of one molecule of ammonia and citrulline in the hydrolase reaction. In contrast to a lateral aspartate in other GME family members that release one molecule of ammonia (Linsky and Fast, 2010), the lateral Asn71 in AgrE-NTD interacts with the NE atom of guanidine group by forming one hydrogen bond (Fig. 10). Therefore, a ~180˚ rotation of the NE–CZ bond in the intermediate following the first release of one ammonia is possible due to the weak interaction of Asn71 with the guanidine group (Tocilj et al., 2005). However, contrary to my expectation, almost two equivalents of ammonia were produced in the enzyme reaction with a higher concentration of the N71D mutant of the AgrE-NTD for several minutes (Fig. 11). Moreover, the mutation of a lateral residue in arginine deiminase into asparagine completely lost enzyme activity, suggesting that there are unknown factors to discriminate between hydrolase and dihydrolase activity.

Figure 9. Binding sites of L-arginine and L-ornithine in the AgrE-NTD

The residues are located within ~4.5 Å of L-ornithine or L-arginine overlaid with $2F_o–F_c$ electron density map contoured at 1.0 σ. The *dashed lines* indicate hydrogen bonds within ~3.2 Å. (A) A zoomed-in view shows L-ornithine bound to the active site in the ternary complex. (B) The binding site of L-arginine in the binary complex of AgrE (C264A) is shown in a zoomed-in view. Asn71 residue is nearer to the NE of L-arginine rather than NH2.

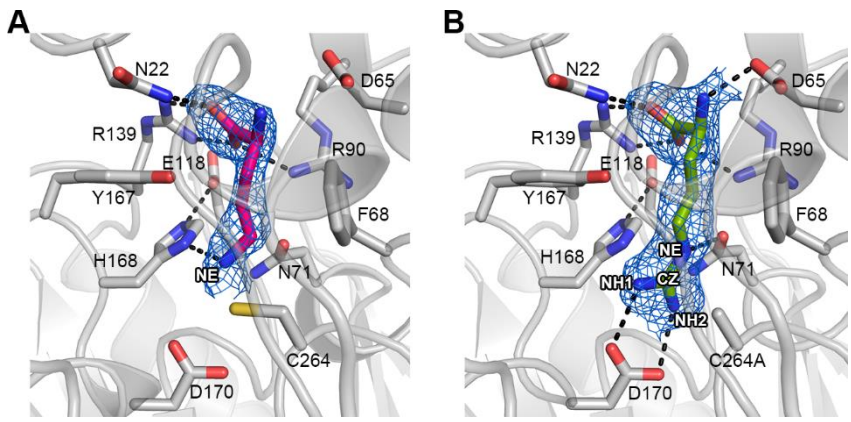
A
N22
D65
R139
R90
E118
Y167
F68
H168
NE
N71
C264
D170
B
N22
D65
R139
R90
E118
Y167
F68
H168
NE
N71
NH1
CZ
NH2
C264A
D170

Figure 10. Comparison of the active sites in hydrolase and dihydrolase in the GME family

(A–B) Dihydrolase. (A) The catalytic triad for the AgrE-NTD is Cys264-His168-Glu118. Its substrate, arginine, was observed in the active site of the AgrE mutant (C264A) (PDB ID 6LRH) (Lee and Rhee, 2020). (B) The substrate *N*-succinylarginine of *N*-succinylarginine dihydrolase is bound to the active site in the C365S mutant (PDB ID 1YNI) (Tocilj et al., 2005). (C–D) Hydrolase. (C) The substrate-bound complex of arginine deiminase from *Pseudomonas aeruginosa* exhibits the binding site of arginine (PDB ID 2A9G) (Galkin et al., 2005). (D) The intermediate is covalently linked with Cys398 as a nucleophile in arginine deiminase from *Mycoplasma arginine* (PDB ID 1S9R) (Das et al., 2004). A water molecule in the reaction is shown in a *red sphere*. Note that an asparagine plays a role of the lateral residue in active sites of dihydrolase while an aspartate serves as the lateral residue in hydrolase enzymes in the GEM family.

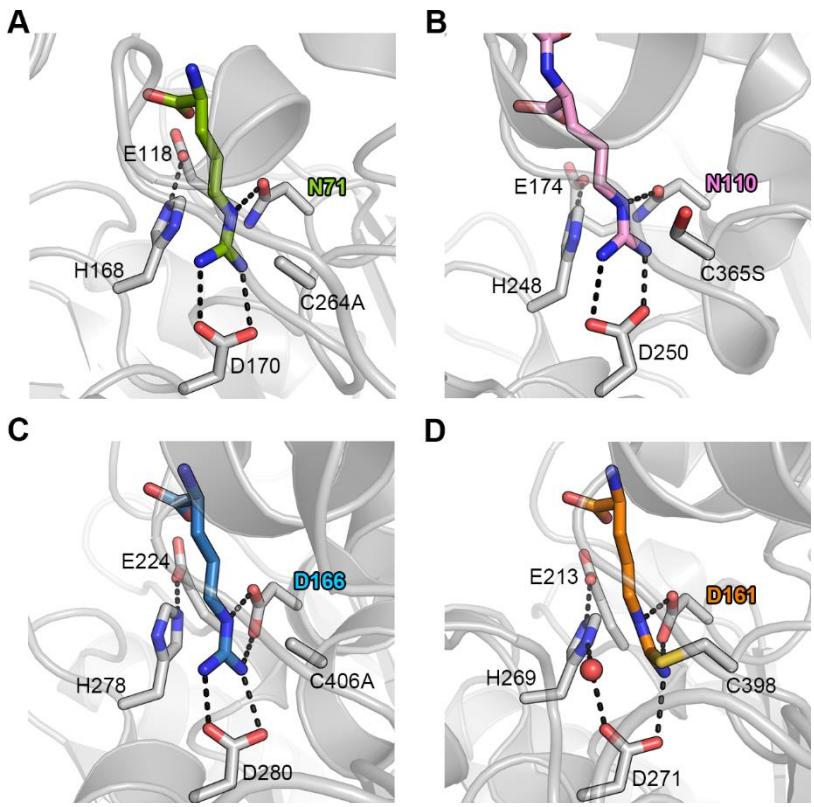
A
E118
N71
H168
C264A
D170
B
E174
N110
H248
C365S
D250
C
E224
D166
H278
C406A
D280
D
E213
D161
H269
C398
D271

Figure 11. Extended reaction for quantitative ammonia production in arginine hydrolase and dihydrolase

The reaction was performed in the presence of arginine (0, 12.5, 25, or 50 μM) and 40 μM of each enzyme at 25℃ over 15 min. (A) The time-course ammonia production is shown in the AgrE-NTD reaction. (B) Arginine deiminase (Galkin et al., 2004) which is a type of arginine hydrolase releasing one ammonia molecule from arginine was cloned from genomic DNA of *Pseudomonas aeruginosa*. The N-terminal His_5-tagged arginine deiminase expressed and purified from *E.coli* was used in the reaction. (C) The N71D mutant of the AgrE-NTD exhibited low activity, but produced more than one ammonia. The reaction was continuous over 20 min. (D) Stoichiometric ammonia production occurred under my assay conditions; two equivalents of ammonia from the AgrE-NTD; one equivalent of ammonia from arginine deiminase.

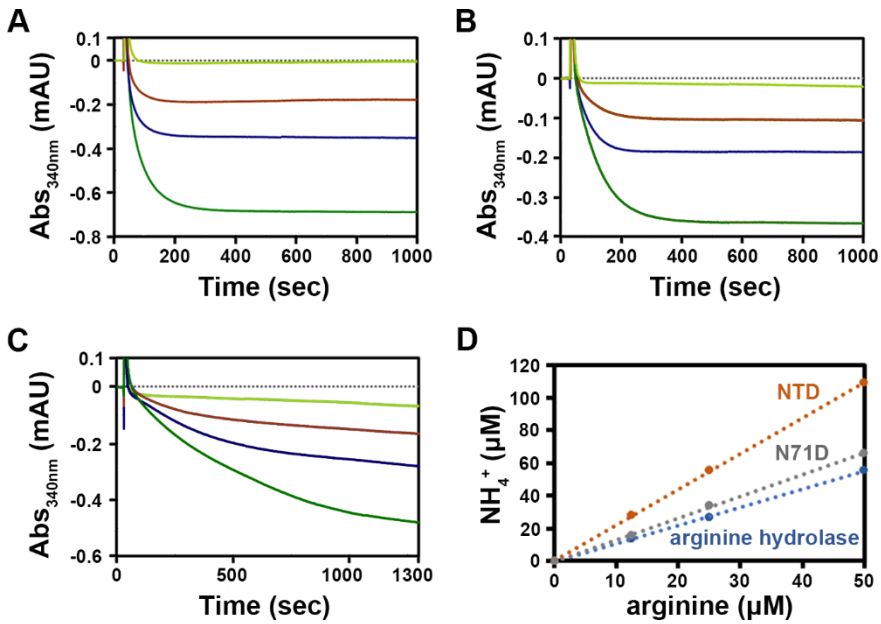
A
B
C
D
Abs340nm (mAU)
Time (sec)
NH4+ (μM)
arginine (μM)
NTD
N71D
arginine hydrolase

Enzyme activity assay of AgrE-NTD

I performed the enzyme activity assay of the AgrE-NTD and its various mutants for arginine dihydrolase activity. First, I validated possible differences of activity between the wild-type AgrE-NTD (Met1 to Val283) and full-length AgrE. The steady-state kinetic analysis indicated that kinetic parameters of the AgrE-NTD and full-length AgrE are similar, but the specific activity of the AgrE-NTD was ~10% higher than that of full-length AgrE (Fig. 12, A and C). It implies that the AgrE-CTD for ornithine cyclodeaminase activity does not affect the NADPH-dependent coupled assay used in this study. Furthermore, I could not characterize the AgrE-CTD activity using full-length AgrE expressed from *E.coli*, as reported previously (Burnat et al., 2019).

For functional analysis, I selected 12 residues in the central hollow of the AgrE-NTD (Fig. 12B). In addition to the residues interacting with L-arginine (Fig. 9B), Asp122 and Asn219 were also additionally selected. These were involved in interactions with water near the core histidine and with the anterior aspartate, respectively. Surprisingly, all mutants exhibited less activity than ~2% of that of the wild-type, except Y167F which showed ~9% of the wild-type activity. According to the analysis, it is indicated that the chemical integrity of residues, besides the catalytic triad, in the active site is significant for arginine dihydrolase activity.

I carried out further kinetic assay for several mutants exhibiting measurable activity with ~100–400-fold higher concentrations of enzymes (Fig. 12C). The D65A and R139A mutants, mediating interactions with the main chain of L-arginine, showed a ~11–25-fold higher K_m and a ~488–586-fold lower k_{cat} than those of wild-type. It is remarkable that N71D, which is equivalent to a lateral aspartate of arginine hydrolase in the GME family, exhibited ~5-fold lower K_m, while the N71A had ~58-fold higher K_m than the wild-type AgrE-NTD. Thus, these observations in this study correspond with the functional roles suggested from structural analysis.

Figure 12. Functional analysis of arginine dihydrolase for the AgrE-NTD

All measurements were conducted in triplicate. (A–B) Specific activity of the AgrE-NTD (Met1 to Val283), full-length AgrE, and various mutants. The error bars indicate standard deviations. In the reaction, 2 mM arginine and 0.2 μM enzymes for full-length AgrE and the AgrE-NTD or mutants with ~10–400-fold higher concentrations were used. Note that a unit of the enzyme used for calculation of specific activity is molar concentration, nM, mainly due to the difference in molecular mass of full-length AgrE and the AgrE-NTD. (C) Steady-state kinetic analysis for the AgrE-NTD, full-length AgrE, D65A, N71A, N71D, and R139A is shown.

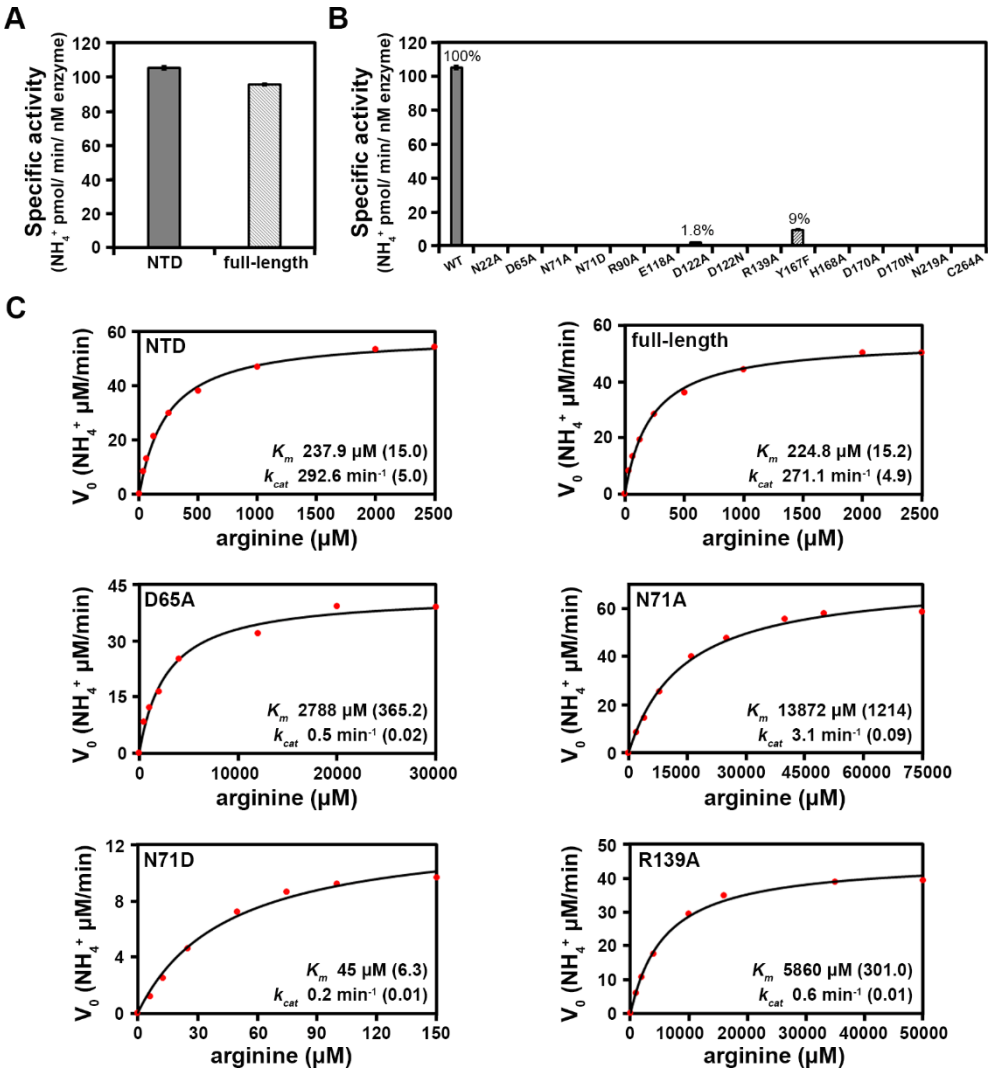
A
Specific activity
(NH4+ pmol/ min/ nM enzyme)
NTD
full-length
B
100%
1.8%
9%
WT
N22A
D65A
N71A
N71D
R90A
E118A
D122A
D122N
R139A
Y167F
H168A
D170A
D170N
N219A
C264A
C
NTD
Km 237.9 μM (15.0)
kcat 292.6 min-1 (5.0)
full-length
Km 224.8 μM (15.2)
kcat 271.1 min-1 (4.9)
D65A
Km 2788 μM (365.2)
kcat 0.5 min-1 (0.02)
N71A
Km 13872 μM (1214)
kcat 3.1 min-1 (0.09)
N71D
Km 45 μM (6.3)
kcat 0.2 min-1 (0.01)
R139A
Km 5860 μM (301.0)
kcat 0.6 min-1 (0.01)
V0 (NH4+ μM/min)
arginine (μM)

NAD(H) binding and substrate channeling of AgrE

In the ternary complex, a cofactor NAD(H) of ornithine cyclodeaminase with a fully extended conformation was bound to the end of the central β-sheet of the AgrE-CTD (Fig. 13A). It is not obvious whether the coenzyme is NADH or NAD^+, considering the $2F_o$-F_c map corresponding to the nicotinamide ring. An loop following the β32 of the central sheet and an α15 following the central β29 strand surround the binding site of the nicotinamide moiety. In particular, the nicotinamide ring is staked with Arg601 in the loop and the main chains of Asn524 and Ala525 in the α15. Two histidine residues, His529 and His557, were also involved in the binding site. Furthermore, Asp603 is within ~3.4 Å from the carboxamide group in the nicotinamide ring.

The binding of the coenzyme NAD(H) to the AgrE-CTD was observed only in one subunit of the dimer. In the tetrameric assembly, each NAD(H) in the dimer was positioned head-to-head in the central AgrE-CTDs, and present at the intersubunit interface (Fig. 13B). Therefore, there are two coenzymes in the tetramer without further steric hindrance in the structural environment in this study. I am not sure whether it is an intrinsic feature of AgrE-CTD or a crystallographic artifact. The substrate L-ornithine of the AgrE-CTD was not observed in my experiments. Also, ornithine cyclodeaminase activity of AgrE-CTD was not detected in the full-length AgrE enzyme expressed from *E.coli* in this assay condition. The truncated construct for AgrE-CTD (Leu358-Gly703) failed to be expressed from *E.coli*. It has been reported previously that the AgrE enzyme expressed from an *Anabaena* strain, but not from *E.coli*, successfully exhibited ornithine cyclodeaminase activity (Burnat et al., 2019).

AgrE as a bifunctional enzyme catalyzes two sequential reactions. The presence of substrate channeling along the active sites between arginine dihydrolase and ornithine cyclodeaminase in AgrE has been proposed (Burnat et al., 2019; Zhang and Yang, 2019). In this study, the structural analysis revealed the substrate channeling

in tetrameric AgrE (Fig. 14), showing an empty space within the molecular surface between the adjacent subunits. Furthermore, the entrance of an active site in the AgrE-NTD is positioned towards the central region of the AgrE-CTDs. In the tetrameric assembly, there are no openings near the binding site of NAD(H) in the AgrE-CTD, thereby suggesting that L-ornithine produced by the AgrE-NTD could be channeled to the AgrE-CTD through the tunnel. As previously described (Burnat et al., 2019), these observations in this study indicate that L-ornithine generated from AgrE-NTD enters a catabolic pathway rather than an arginine synthetic pathway as a substrate (Zhang et al., 2018) under certain favoring conditions for arginine catabolism. Moreover, the bifunctional enzyme PutA also employed substrate channeling to produce glutamate in the AgrE–PutA pathway (Liu et al., 2017).

Figure 13. Binding site of coenzyme NAD(H) in the AgrE-CTD

(A) The coenzyme NAD(H) for ornithine cyclodeaminase was bound on the Rossmann fold of the AgrE-CTD, with a $2F_o–F_c$ electron density map contoured at 1.0 σ. The *dashed lines* represent hydrogen bonds, and the residues forming possible pocket for the nicotinamide moiety are shown. This figure was produced using monomeric AgrE. (B) Surface of the binding site for coenzyme NAD(H) in tetrameric AgrE is represented. Each subunit is displayed by different color as exhibited in Fig. 6B.

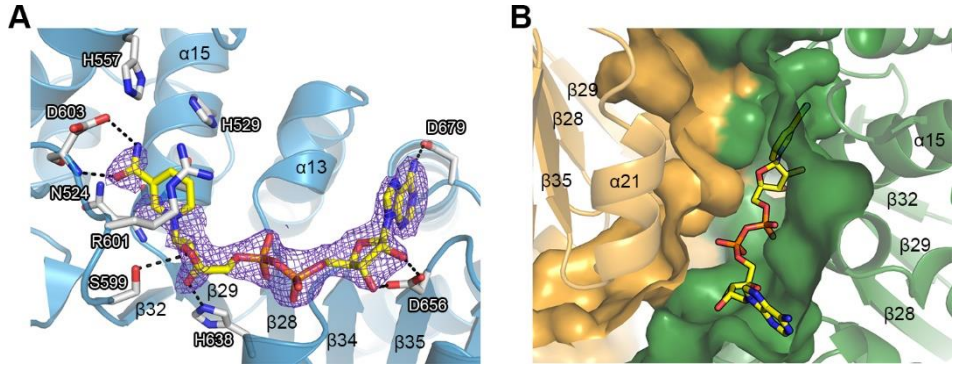
A
H557
α15
D603
H529
D679
α13
N524
R601
S599
β29
β32
D656
H638
β28
β34
β35
B
β29
β28
α15
β35
α21
β32
β29
β28

Figure 14. Substrate channeling

(A) An inter-subunit space is displayed in the ternary complex. The inner area filled by the enzyme is shown in *dark gray*, and different color of each subunit as exhibited in Fig. 6B represents the molecular envelope. There is an empty space between L-ornithine and NAD(H), which serves as a tunnel for substrate channeling. (B) The substrate tunnel is shown in a zoomed-in view. L-ornithine is isolated in the ternary complex, mainly due to the loop (*blue*) orientation.

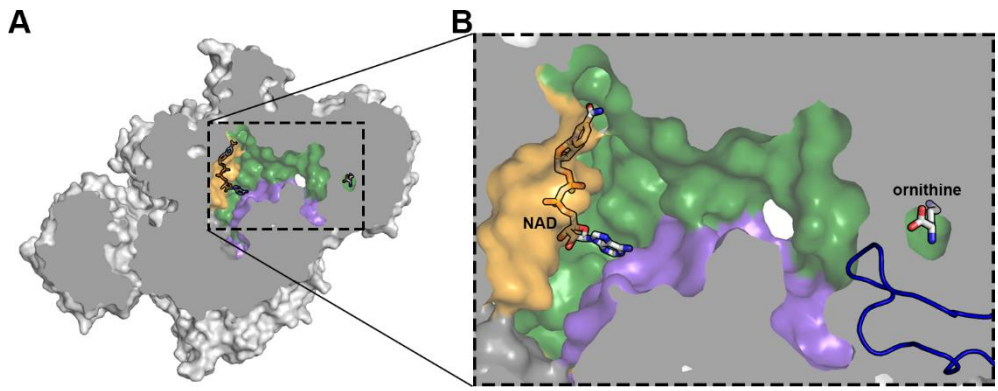
A
B
NAD
ornithine

Discussion

In this study, I performed structural and functional analyses for the AgrE enzyme with its various mutants from the cyanobacterium *Anabaena*. The tetrameric AgrE is a bifunctional enzyme involved in the catabolic pathway of arginine degraded from cyanophycin and converts arginine into three molecules of ammonia, CO_2, and proline with ornithine as an intermediate. Arginine catabolism plays a significant role in nitrogen mobilization in cyanobacteria that can synthesize cyanophycin as a reservoir of fixed nitrogen.

The bifunctional AgrE enzyme includes arginine dihydrolase activity and ornithine cyclodeaminase activity in the AgrE-NTD and the AgrE-CTD, respectively. The AgrE-NTD has a five-fold α/β propeller which is conserved in the GME family, and the catalytic triad in the active site of the AgrE-NTD consists of Cys264, His168, and Glu118. The AgrE-CTD has two subdomains including a Rossmann fold for the coenzyme NAD(H) binding site.

I determined the three crystal structures of AgrE including an unliganded SeMet–substituted structure, a ternary complex with L-ornithine as a product in the AgrE-NTD and the coenzyme NAD(H) in the AgrE-CTD, and a binary complex with L-arginine as a substrate in the AgrE-NTD. The structural analysis in this study revealed the binding sites for the substrate of arginine dihydrolase and the coenzyme of ornithine cyclodeaminase. However, I couldn't determine the AgrE complex with the substrate and product of ornithine cyclodeaminase. Furthermore, the ornithine cyclodeaminse activity in the AgrE enzyme expressed from *E.coli* was not detected in my enzymatic assay conditions. Given these studies, there might be another unknown factor in *Anabaena* essential for the ornithine cyclodeaminase activity of AgrE. DALI search (Holm and Laakso, 2016) suggested that the structure of AgrE-CTD is similar with SIRT6, NAD-dependent deacetylase with a Rossmann fold,

which has an distinct site for an allosteric activator (PDB ID 5Y2F) (Huang et al., 2018).

In addition to the catalytic triad in the AgrE-NTD, Asn71 as a lateral residue and Asp170 as an anterior residue mediate interactions with the guanidine group of L-arginine. It has been proposed previously that the lateral asparagine residue would rotate the NE-CZ bond of the guanidine group for the dihydrolase activity (Tocilj et al., 2005), and the detail of arginine dihydrolase mechanism was recently proposed on the ArgZ study (Zhuang et al., 2020). In my functional analysis on the AgrE-NTD, N71D mutant exhibited ~5-fold lower K_m than that of the wild-type. It indicates that the lateral asparagine rather than aspartate mediates weaker interactions with L-arginine, supporting the proposed key role of Asn71 in the catalytic mechanism for arginine dihydrolase.

In the tetrameric assembly of AgrE, the binding of coenzyme NAD(H) in the AgrE-CTD for ornithine cyclodeaminase revealed that there is possible substrate channeling between L-arginine in the AgrE-NTD and the nicotinamide ring of NAD(H) in AgrE-CTD with a distance of ~45 Å.

Taken together, these analyses in this study give structural and functional insights into AgrE required for arginine catabolism in *Anabaena* sp. strain PCC 7120. The bifunctional enzyme AgrE catalyzes two consecutive reactions which produce ammonia and proline from arginine, followed by producing glutamate by PutA enzyme for nitrogen mobilization. It was reported previously that the *agrE* as well as *putA* gene is widely present in cyanobacteria that produce cyanophycin (Burnat et al., 2019). The results in this study identifying a role of Asn71 for arginine dihydrolase activity and substrate channeling in AgrE could support the role of AgrE responsible for nitrogen mobilization in cyanobacteria through catabolism of arginine degraded from cyanophycin.

References

Adams PD, Afonine PV, Bunkóczi G, Chen VB, Davis IW, Echols N et al. (2010) PHENIX: a comprehensive python-based system for macromolecular structure solution. *Acta Crystallogr D Biol Crystallogr* 66, 213–221

Allen MM, Hutchison F, and Weathers PJ (1980) Cyanophycin granule polypeptide formation and degradation in the cyanobacterium *Aphanocapsa* 6308. *J Bacteriol* 141, 687–693

Burnat M, Herrero A, and Flores E (2014) Compartmentalized cyanophycin metabolism in the diazotrophic filaments of a heterocyst-forming cyanobacterium. *Proc Natl Acad Sci USA* 111, 3823–3828

Burnat M, Picossi S, Valladares A, Herrero A, and Flores E (2019) Catabolic pathway of arginine in *Anabaena* involves a novel bifunctional enzyme that produces proline from arginine. *Mol Microbiol* 111, 883–897

Das K, Butler GH, Kwiatkowski V, Clark Jr AD, Yadav P, and Arnold E (2004) Crystal structures of arginine deiminase with covalent reaction intermediates; implications for catalytic mechanism. *Structure* 12, 657–667

Diederichs K and Karplus PA (2013) Better models by discarding data? *Acta Crystallogr D Biol Crystallogr* 69, 1215–1222

Emsley P, Lohkamp B, Scott WG, and Cowtan K (2010) Features and development of Coot. *Acta Crystallogr D Biol Crystallogr* 66, 486–501

Flores E and Herrero A (2010) Compartmentalized function through cell differentiation in filamentous cyanobacteria. *Microbiology* 8, 39–50

Galkin A, Kulakova L, Sarikaya E, Lim K, Howard A, and Herzberg O (2004) Structural insights into arginine degradation by arginine deiminase, an antibacterial and parasite drug target. *J Biol Chem* 279, 14001–14008

Galkin A, Lu X, Dunaway-Mariano D, and Herzberg O (2005) Crystal structures representing the michaelis complex and the thiouronium reaction intermediate of *Pseudomonas aeruginosa* arginine deiminase. *J Biol Chem* 280, 34080–34087

Goodman JL, Wang S, Alam S, Ruzicka FJ, Frey PA, and Wedekind JE (2004) Ornithine Cyclodeaminase: structure, mechanism of action, and implications for the μ-crystallin family. *Biochemistry* 43, 13883-13891

Hejazi M, Piotukh K, Mattow J, Deutzmann R, Volkmer-Engert R, and Lockau W (2002) Isoaspartyl dipeptidase activity of plant-type asparaginases. *Biochem J* 364, 129–136

Holm L and Laakso LM (2016) Dali server update. *Nucleic Acids Res* 44, W351–W355

Huang Z, Zhao J, Deng W, Chen Y, Shang J, Song K et al. (2018) Identification of a cellularly active SIRT6 allosteric activator. *Nat Chem Biol* 14, 1118–1126

Karplus PA and Diederichs K (2012) Linking crystallographic model and data quality. *Science* 336, 1030–1033

Krissinel E and Henrick K (2007) Inference of macromolecular assemblies from crystalline state. *J Mol Biol* 372, 774–797

Lee H and Rhee S (2020) Structural and mutational analyses of the bifunctional arginine dihydrolase and ornithine cyclodeaminase AgrE from the cyanobacterium *Anabaena*. *J Biol Chem* 295, 5751–5760

Linsky T and Fast W (2010) Mechanistic similarity and diversity among the guanidine-modifying members of the pentein superfamily. *Biochim Biophys Acta* 1804, 1943–1953

Liu L-K, Becker DF, and Tanner JJ (2017) Structure, function, and mechanism of proline utilization A (PutA). *Arch Biochem Biophys* 632, 142–157

Murray-Rust J, Leiper J, McAlister M, Phelan J, Tilley S, Santa Maria J et al. (2001) Structural insights into the hydrolysis of cellular nitric oxide synthase inhibitors by dimethylarginine dimethylaminohydrolase. *Nat Struct Biol* 8, 679–683

Muro-Pastor MI, Reyes JC, and Florencio FJ (2005) Ammonia assimilation in cyanobacteria. *Photosynth Res* 83, 135–150

Otwinowski Z and Minor W (1997) Processing of X-ray diffraction data collected in oscillation mode. *Methods Enzymol* 276, 307–326

Richter R, Hejazi M, Kraft R, Ziegler K, and Lockau W (1999) Cyanophycinase, a peptidase degrading the cyanobacterial reserve material multi-L-arginyl-poly-L-aspartic acid (cyanophycin). *Eur J Biochem* 263, 163–169

Robert X and Gouet P (2014) Deciphering key features in protein structures with the new ENDscript server. *Nucleic Acids Res* 42, W320–W324

Simon RD (1973) The effect of chloramphenicol on the production of cyanophycin granule polypeptide in the blue-green alga *Anabaena cylindrica*. *Arch Microbiol* 92, 115–122

Simon RD and Weathers P (1976) Determination of the structure of the novel polypeptide containing aspartic acid and arginine which is found in cyanobacteria. *Biochim Biophys Acta* 420, 165–176

Tocilj A, Schrag JD, Li Y, Schneider BL, Reitzer L, Matte A et al. (2005) Crystal structure of *N*-succinylarginine dihydrolase AstB, bound to substrate and product, an enzyme from the arginine catabolic pathway of *Escherichia coli*. *J Biol Chem* 280, 15800–

15808

Van Duyne GD, Standaert RF, Karplus PA, Schreiber SL, Clardy J (1993) Atomic structures of the human immunophilin FKBP-12 complexes with FK506 and rapamycin. *J Mol Biol* 229, 105–124

Winn MD, Ballard CC, Cowtan KD, Dodson EJ, Emsley P, Evans PR et al. (2011) Overview of the CCP4 suite and current developments. *Acta Crystallogr D Biol Crystallogr* 67, 235–242

Zehr JP (2011) Nitrogen fixation by marine cyanobacteria. *Trends Microbiol* 19, 162–173

Zhang H and Yang C (2019) Arginine and nitrogen mobilization in cyanobacteria. *Mol Microbiol* 111, 863–867

Zhang H, Liu Y, Nie X, Liu L, Hua Q, Zhao G-P et al. (2018) The cyanobacterial ornithine–ammonia cycle involves an arginine dihydrolase. *Nat Chem Biol* 14, 575–581

Zhuang N, Zhang H, Li L, Wu X, Yang C, and Zhang Y (2020) Crystal structures and biochemical analyses of the bacterial arginine dihydrolase ArgZ suggests a "bond rotation" catalytic mechanism. *J Biol Chem* 295, 2113–2124

Zwart PH, Gross-Kunstleve RW, and Adams PD (2005) Xtriage and Fest: automatic assessment of X-ray data and substructure structure factor estimation. *CCP4 Newsletter* 42, 10

초 록

시아노박테리아 아나베나 유래 두 가지 기능 보유 효소 AgrE의 구조와 기능에 대한 연구

서울대학교 대학원

농생명공학부 응용생명화학전공

이해희

아르기닌은 질소 함유량이 높은 아미노산으로, 시아노박테리아에서 아르기닌 대사 경로는 질소의 순환과 저장에 중요한 역할을 한다. 시아노박테리아 *Anabaena* sp. strain PCC 7120와 *Synechocystis* sp. PCC 6803에서 유래한 AgrE와 ArgZ는 최근에 알려진 효소로, 이들의 N 말단 도메인은 guanidine-modifying enzyme family (GME family)에 속하는 arginine dihydrolase 이다. 이 효소들은 아르기닌을 분해하는 경로를 촉진하며 오르니틴과 이산화탄소 뿐만 아니라 암모니아를 생성한다. *Synechocystis* sp. PCC 6803에서 ArgZ에 의한 오르니틴–암모니아 회로는 질소의 재순환과 질소의 저장에 관여한다. AgrE의 C 말단 도메인은 ornithine cyclodeaminase 기능을 가지고 있으며 오르니틴을 프롤린과 암모니아로 전환시킨다. 따라서, AgrE는 두 개의 연속적인 반응을 통해 아르기닌 이화작용에 관여하는 두가지 기능을 가진 효소이다. 본 논문에서는 AgrE의 구조 연구를 통해 AgrE가 사합체로 존재하는 것을 확인했고,

AgrE의 복합체 구조를 통해 N 말단 도메인에 arginine dihydrolase의 기질인 아르기닌과 생성물인 오르니틴이 결합하는 부위를 밝혀냈다. 또한, N 말단 도메인에 오르니틴과 C 말단 도메인에 ornithine cyclodeaminase의 조효소인 NAD(H)가 결합한 사합체 구조를 통해서 N 말단과 C 말단 도메인의 활성부위 사이에 AgrE 효소 반응의 중간산물인 오르니틴이 이동할 수 있는 기질 채널링 통로를 밝혀냈다. 그러나 본 논문에서 사용된 대장균에서 발현시킨 AgrE는 ornithine cyclodeaminase의 기능을 보이지 않았다. 본 논문에서는 N 말단 도메인의 다양한 돌연변이체를 이용한 기능 분석을 통해 같은 GME family의 arginine hydrolase와 차별되는 arginine dihydrolase의 기능에 중요한 잔기를 밝혀냈다.

주요어: *Anabaena* sp. strain PCC 7120, 암모니아 생성, arginine catabolism, bifunctional enzyme, guanidine removing enzyme, nitrogen remobilization, substrate channeling, X-ray crystallography

학 번: 2018-21199